

ON CONTACT BETWEEN CURVES AND RIGID SURFACES – FROM VERIFICATION OF THE EULER-EYTELWEIN PROBLEM TO KNOTS

ALEXANDER KONYUKHOV*, KARL SCHWEIZERHOF† AND
ANDREAS METZGER†

*Institute of Mechanics
Karlsruhe Institute of Technology
Kaiserstrasse 12, 76131 Karlsruhe, Germany
e-mail: Alexander.Konyukhov@kit.edu, http://www.ifm.kit.edu/14_203.php/

†Institute of Mechanics
Karlsruhe Institute of Technology
Kaiserstrasse 12, 76131 Karlsruhe, Germany
<http://www.ifm.kit.edu/>

Key words: Curve-To-Curve Contact, Curve-To-Surface contact, Euler-Eytelwein Problem, Belt Friction Problem, Knots

Abstract. A general theory for the Curve-To-Curve contact is applied to develop a special contact algorithm between curves and rigid surfaces. In this case contact kinematics are formulated in the local coordinate system attached to the curve, however, contact is defined at integration points of the curve line (Mortar type contact). The corresponding Closest Point Projection (CPP) procedure is used to define then a shortest distance between the integration point on a curve and the rigid surface. For some simple approximations of the rigid surface closed form solutions are possible. Within the finite element implementation the isogeometric approach is used to model curvilinear cables and the rigid surfaces can be defined in general via NURB surface splines. Verification of the finite element algorithm is given using the well-known analytical solution of the Euler-Eytelwein problem – a rope on a cylindrical surface. The original 2D formula is generalized into the 3D case considering an additional parameter H -pitch for the helix. Finally, applications to knot mechanics are shown.

1 INTRODUCTION

In many engineering devices such capstan and belt drives frictional interaction between structure and ropes, cables or belts can be modeled as the interaction between rigid surfaces and deformable curvilinear beams or ropes without loss of tolerance. Several

developments are required for this problem: a robust cable finite element and a contact algorithm for the Curve-To-Rigid Surface contact interaction. The isogeometric approach, see [1], is employed together with a special finite beam element formulation allowing both finite rotations, see in [2] in order to obtain cable finite elements. The theory for Curve-To-Curve contact interaction developed in [3] is applied to obtain a contact algorithm describing the contact between a deformable curve (representing either the center-line of the beam or an edge of a solid body) and a rigid surface.

The classical Euler-Eytelwein solution of the belt friction problem, see e.g. in [4], is first employed to verify the developed algorithm. The solution of this problem was reported by Euler in his *Remarks on the effect of friction on equilibrium* and has been first published by the Berlin Academy of science [5] in 1769. Since the first time publishing the Euler solution by Eytelwein [6] in his *Handbuch der Statik fester Körper* in 1808 the problem is spread through the practical applications and became known as Euler-Eytelwein problem in many books of technical mechanics. Here we are proposing a generalization of the classical 2D solution into the 3D case under the assumption that the rope is forming a spiral line on a rigid cylinder. This solution in due course is used for verification.

Finally, combination of both Curve-To-Curve and Curve-To-Rigid Surface contact algorithms allows to step into modeling of more complex see-man knots (beginning of study see in [7]) such as the clove-hitch knot. Numerical examples are illustrating the tying-up-processes.

2 CURVE-TO-RIGID ANALYTICAL SURFACE CONTACT ALGORITHM

The theory for Curve-To-Curve contact developed in [3] is employed to obtain a contact algorithm between a deformable curve and a rigid surface as follows. A rigid surface is assumed to have arbitrary analytical description, e.g. via NURBS surfaces. All contact parameters for the Curve-To-Rigid Surface algorithm are defined similar to the Curve-To-Curve contact algorithm in the Serret-Frenet frame, see [3], obtained by the tangent vector $\boldsymbol{\tau}$, the normal vector $\boldsymbol{\nu}$ and the bi-normal $\boldsymbol{\beta}$ of the curve line, see Fig. 1. A vector \mathbf{e} is defining the shortest distance.

In order to describe contact between deformable curves and rigid surfaces a Segment-To-Analytical-Surface (STAS) algorithm, discussed in [9], is modified using the projection of the integration points which is set up on the “slave” curve onto the rigid “master” surface. The combination of this strategy with the Curve-To-Rigid (analytical) Surface contact algorithm leads to the following definition of the coordinate system on the master surface:

$$\boldsymbol{\rho}_s(\xi) = \mathbf{r}(\alpha_1, \alpha_2) + p\mathbf{n}(\alpha_1, \alpha_2), \quad (1)$$

where $\boldsymbol{\rho}_s(\xi)$ is defining an integration point positioned on the mid-line of the curvilinear beam element, $\mathbf{r}(\alpha_1, \alpha_2)$ is parameterization of the rigid “master” surface. The integration point $\boldsymbol{\rho}_s(\xi)$ is found in the direction of the normal $\mathbf{n}(\alpha_1, \alpha_2)$ to the rigid “master” surface. The shortest distance between integration points and the surface denoted as p plays

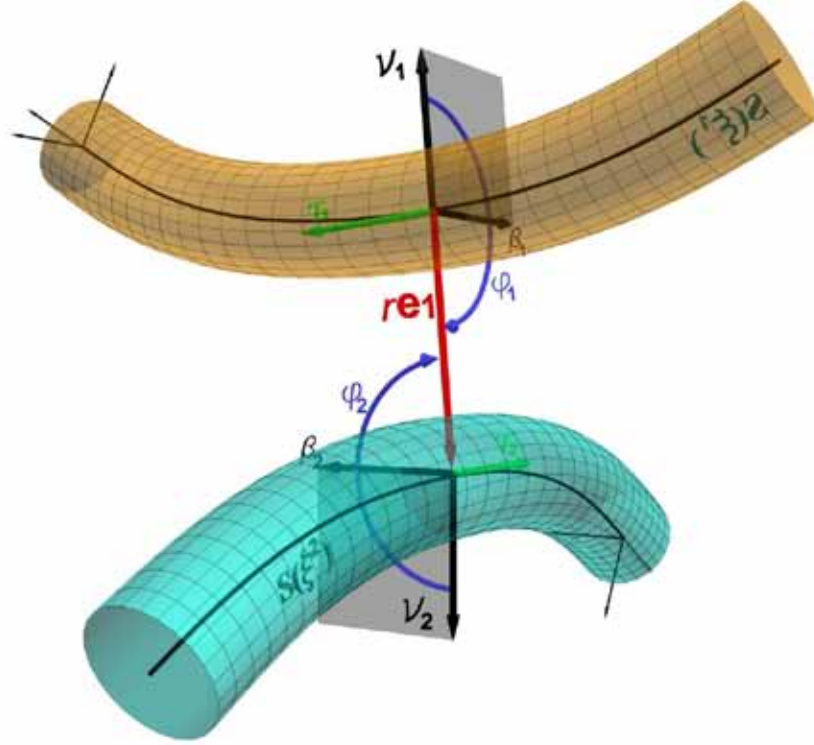


Figure 1: Curve-To-Curve contact algorithm is defined in the Serret-Frenet frame for both curves.

the role of a penetration. The Closest Point Projection (CPP) procedure, which is the standard contact local searching algorithm now turns into the determination of the surface convective coordinates α_1, α_2 defined by equation (1). In general, Newtons method is exploited to solve eqn. (1) defining then a point on the rigid surface and the penetration p between this surface and the selected integration point S . An analytical solution is possible for some surfaces – one of the important examples for further verification is the contact of a curve with a rigid cylindrical surface. Here, the rigid cylindrical surface with the radius R is given as $\mathbf{r} = \mathbf{R}_C + z\mathbf{e}_z + R\mathbf{e}_\varphi(\varphi)$ with the normal vector $\mathbf{n} = \mathbf{e}_\varphi(\varphi)$, see Fig. 2.

The distance p and thereby penetration into the cylinder is defined as

$$p = \begin{cases} \|\mathbf{R}_C - \boldsymbol{\rho}_s - ((\mathbf{R}_C - \boldsymbol{\rho}_s) \cdot \mathbf{e}_z) \mathbf{e}_z\| - R & \text{for an outward normal} \\ R - \|\mathbf{R}_C - \boldsymbol{\rho}_s - ((\mathbf{R}_C - \boldsymbol{\rho}_s) \cdot \mathbf{e}_z) \mathbf{e}_z\| & \text{for an inward normal} \end{cases} \quad (2)$$

It should be noticed that for the contact between the cylinder and a cable with a circular cross-section with radius R_{cable} , the penetration is, of course, computed as $penetration = p - R_{cable}$.

A coordinate z is used as a measure of tangential interactions for the definition of frictional interaction.

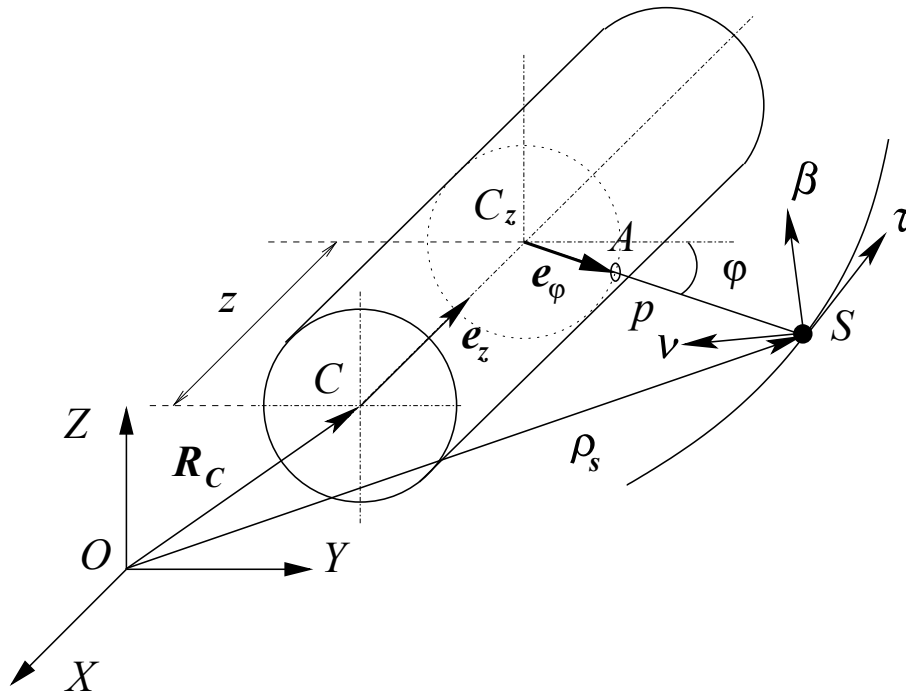


Figure 2: Contact with a rigid cylinder given by an analytical equation.

The contact integral is representing then the virtual work of contact traction along the curve L and is computed numerically using the integration formula of Lobatto or Gauss type depending on modeling purposes. Thus, e.g. the part responsible only for the normal contact is represented by

$$\delta W = \int_L N \delta p ds. \quad (3)$$

For the derivation of tangent matrices results from the Curve-To-Curve contact approach, see in [3], are employed directly. Thus, the tangent matrix derived from the linearized part of eqn. (3) is given as

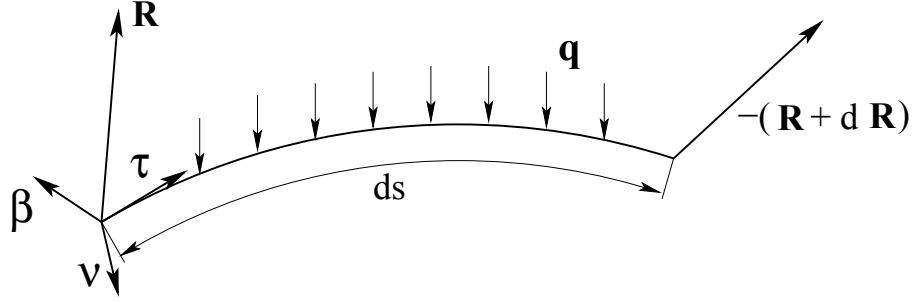
$$\mathbf{K}^N = \int_L \varepsilon_r \mathbf{A}^T [\mathbf{e} \otimes \mathbf{e}] \mathbf{A} ds \quad (4a)$$

$$+ \int_L N \mathbf{A}^T \left\{ \frac{k \cos \varphi_1}{(1 - rk \cos \varphi)} \boldsymbol{\tau} \otimes \boldsymbol{\tau} - \frac{1}{r} \mathbf{g} \otimes \mathbf{g} \right\} \mathbf{A} ds. \quad (4b)$$

Here, N is a normal contact force, ε_r is a normal penalty parameter, \mathbf{e} is a vector defining the shortest distance, $\mathbf{g} = \boldsymbol{\tau} \times \mathbf{e}$ is an orthogonal vector, r is the shortest distance between the integration point and the rigid surface, k is the curvature of the curve, φ is the angle between the normal curve vector $\boldsymbol{\nu}$ and the unit vector of the shortest distance \mathbf{e} ($\mathbf{e} = \mathbf{e}_1$ in Fig. 1 and $\mathbf{e} = -\mathbf{e}_\varphi$ in Fig. 2). For all geometrical parameters see Fig. 1. \mathbf{A} is an approximation operator for the curve line. The frictional tangential force T is computed

via the return-mapping algorithm. For the derivation of the tangential force T and other parameters including the tangent matrices and more details see [3].

3 GENERALIZATION OF THE EULER-EYTELWEIN FORMULA INTO THE 3D CASE CONSIDERING PITCH H



The equilibrium equation of the elementary part of the rope with length ds , see Fig. 3, is given in the following vector form

$$\frac{d\mathbf{R}}{ds} = \mathbf{q} \quad (5)$$

The force vector \mathbf{R} can be expanded in the natural Serret-Frenet coordinate system used in the differential geometry of curves, see e.g. in [8], built by the unit tangent $\boldsymbol{\tau}$, the unit normal $\boldsymbol{\nu}$ and the unit bi-normal $\boldsymbol{\beta}$ vectors

$$\mathbf{R} = T\boldsymbol{\tau} + N\boldsymbol{\nu} + B\boldsymbol{\beta}, \quad (6)$$

with T – a tangential force, N – a normal force, and B – a bi-normal force. The full derivative of the force vector includes also a part due to changing the basis vectors $\boldsymbol{\tau}$, $\boldsymbol{\nu}$, $\boldsymbol{\beta}$ and is obtained via the Serret-Frenet formula, see e.g. in [8] and the application for this problem in [11]. Taking this formula into account, the projection of eqn. (5) onto the axes $\boldsymbol{\tau}$, $\boldsymbol{\nu}$, $\boldsymbol{\beta}$ results then in the system of ordinary differential equations:

$$\begin{cases} \frac{dT}{ds} + kN &= q_\tau \text{ – equilibrium in } \boldsymbol{\tau} \text{ direction} \\ \frac{dN}{ds} - kT + \varkappa B &= q_\nu \text{ – equilibrium in } \boldsymbol{\nu} \text{ direction} \\ \frac{dB}{ds} - \varkappa N &= q_\beta \text{ – equilibrium in } \boldsymbol{\beta} \text{ direction} \end{cases} \quad (7)$$

where k is the curvature and \varkappa is the torsion of the curve, which are in general functions of the arc-length parameter s .

3.1 Solution of the equilibrium equation for a spiral line (helix)

Now we consider a special case with the following conditions:

- (i) the rope is positioned on the rigid surface.
- (ii) the rope is loaded only by tangential forces $T_0\boldsymbol{\tau}_0$ and $T_1\boldsymbol{\tau}_1$ at both ends.
- (iii) the rope is beginning to slide preserving its geometrical shape, i.e. only a motion along $\boldsymbol{\tau}$ is possible. Thus the form of the helix is conserved.
- (iv) sliding is subjected to the Coulomb friction law such that $T(s) = \mu N(s)$, where μ is a coefficient of friction.

Thus, due to condition (iii), the first equilibrium equation in (7) is transferred into the equation of motion according to D'Alemberts principle with

$$q_\tau = -\rho \frac{\partial^2 u}{\partial t^2}, \quad (8)$$

where u is a tangential component of the displacement and ρ is the linear mass density. However, equilibrium along $\boldsymbol{\nu}$ and $\boldsymbol{\beta}$ axis is fulfilled and we consider the absence of the distributed forces $q_\nu = 0$, $q_\beta = 0$. The problem is then described by the system of ordinary differential equations:

$$\begin{cases} \frac{dN}{ds} - kT + \varkappa B = 0 \\ \frac{dB}{ds} - \varkappa N = 0 \end{cases} \quad (9)$$

with the following initial conditions at $s = 0$ resulting from condition (ii):

$$T(0) = T_0, \quad N(0) = N_0, \quad B(0) = 0. \quad (10)$$

Now, we consider a case with a constant curvature k and a constant torsion \varkappa of the curve. This is a case of the spiral line – a helix – on the cylinder. The system of equations (9) is transformed into a single differential equation of second order by taking the derivative of the first equation in (9):

$$\frac{d^2 N}{ds^2} - k \frac{dT}{ds} + \varkappa \frac{dB}{ds} = 0 \quad (11)$$

and then using the second equation in (9) we obtain

$$\frac{d^2 N}{ds^2} - k \frac{dT}{ds} + \varkappa^2 N = 0. \quad (12)$$

Now taking into account the sliding condition (iv) we obtain a second order differential equation :

$$\frac{d^2 N}{ds^2} - \mu k \frac{dN}{ds} + \varkappa^2 N = 0 \quad (13)$$

with the initial conditions:

$$N(0) = N_0, \quad \frac{dN(0)}{ds} = kT_0. \quad (14)$$

The solution of the ordinary differential equation (13) is obtained by using the characteristic equation

$$\lambda^2 - \mu k \lambda + \varkappa^2 = 0 \quad (15)$$

$$\lambda_{1,2} = \frac{\mu k \pm \sqrt{\mu^2 k^2 - 4\varkappa^2}}{2} \quad (16)$$

Depending on the determinant $D = \mu^2 k^2 - 4\varkappa^2$ three solutions are possible. We consider these values for the spiral line (helix). The geometrical characteristics for this line are defined as follows, see Fig. 3

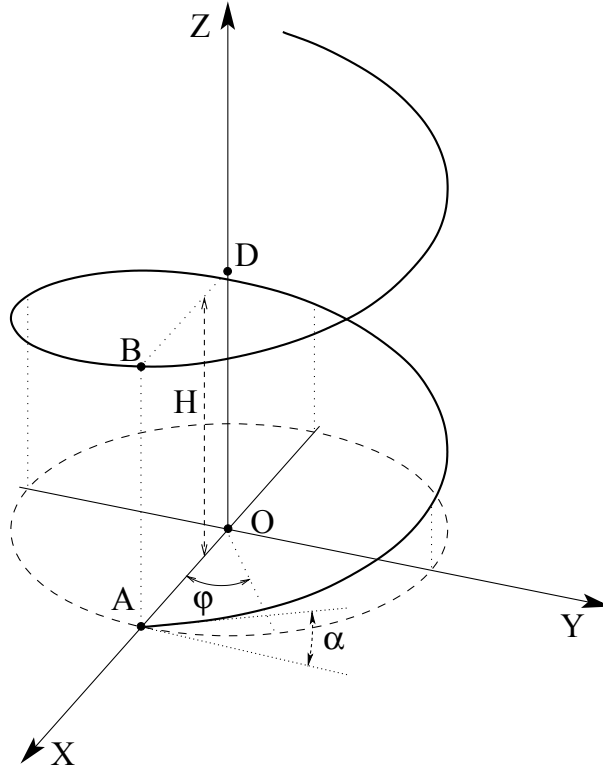


Figure 3: Spiral line (helix) with a pitch H .

Parametrization of the spiral line (helix):

$$\mathbf{r} = \left\{ \begin{array}{c} R \cos \varphi \\ R \sin \varphi \\ \frac{H}{2\pi} \varphi + \text{const} \end{array} \right\}. \quad (17)$$

Within $0 \leq \varphi \leq 2\pi$ the line is making a full turn around the OZ -axis raising by the pitch $z = H$ with the following geometrical items: arc-length of the spiral line (helix) $s = \sqrt{R^2 + \left(\frac{H}{2\pi}\right)^2} \varphi$, $\varphi \in [0, \dots]$; curvature of the helix $k = \frac{R}{R^2 + \left(\frac{H}{2\pi}\right)^2}$; torsion of the

spiral line (helix) $\varkappa = \frac{H/2\pi}{R^2 + \left(\frac{H}{2\pi}\right)^2}$. Then positivity of the determinant can be expressed via the geometrical parameters of the helix as

$$D \geq 0 \implies \mu k \geq 2\varkappa \implies \mu \geq \frac{H}{\pi R}. \quad (18)$$

Omitting details of transformations we discuss the expressions for the force ratio $\frac{T}{T_0}$ for all three possible cases.

3.1.1 Case 1. Positive determinant $D > 0$, $\mu > \frac{H}{\pi R}$

Since with $H = 0$ the determinant is positive $D > 0$, then this case is representing a spiral line with a very small pitch H in comparison with the radius R . The solution is given by the exponential functions as:

$$\frac{T}{T_0} = \left(\frac{\mu k}{2\omega} \sinh \omega s + \cosh \omega s \right) e^{\frac{\mu k}{2}s}, \quad (19)$$

with ω

$$\omega = \frac{\sqrt{\mu^2 k^2 - 4\varkappa^2}}{2}. \quad (20)$$

If we consider the 2D case with $H = 0$ in eqn. (19) **the classical Euler-Eytelwein for the rope on the cylinder is recovered**

$$\frac{T}{T_0} = \left[\sinh \left(\frac{\mu \varphi}{2} \right) + \cosh \left(\frac{\mu \varphi}{2} \right) \right] e^{\frac{\mu \varphi}{2}} = e^{\mu \varphi}. \quad (21)$$

3.1.2 Case 2. Negative determinant $D < 0$, $\mu < \frac{H}{\pi R}$

The case is representing either a case with a spiral line with large pitch H , or with a small coefficient of friction. The solution is given by the trigonometrical and exponential functions:

$$\frac{T}{T_0} = \left[\frac{k\mu}{2\tilde{\omega}} \sin \tilde{\omega}s + \cos \tilde{\omega}s \right] e^{\frac{\mu k}{2}s}, \quad (22)$$

with $\tilde{\omega}$

$$\tilde{\omega} = \frac{\sqrt{4\pi^2 - \mu^2 k^2}}{2}. \quad (23)$$

3.1.3 Limit case 3. Determinant is zero $D = 0$, $\mu = \frac{H}{\pi R}$

This case can be obtained just by the limit process with $\omega \rightarrow 0$ with the solution in eqn. (19) or in eqn. (22) as

$$\lim_{\omega \rightarrow 0} \frac{T}{T_0} = \left[\frac{k\mu}{2}s + 1 \right] e^{\frac{\mu k}{2}s}. \quad (24)$$

A numerical computation for the cases with $D > 0$, $D = 0$, $D < 0$ and the classical Euler formula with $H = 0$ is presented in Fig. 4 for the angle $\varphi \in [0, 2\pi]$. The computation is given with a coefficient of friction $\mu = 0.3$ and radius $R = 1.0$ for the following cases:

- Classical Euler case $H = 0$;
- Positive determinant $D < 0$ with $H = 0.75$
- Zero determinant $D = 0$ with $H = \mu\pi R = 0.9424$
- Negative determinant $D < 0$ with $H = 1.2$

One can see, that if the pitch H is increasing then the ratio of forces T/T_0 is decreasing, thus, the standard 2D Euler case is representing the upper limit of the forces ratio T/T_0 with regard to the pitch H .

The derived formula is used further for the verification of the Curve-To-Rigid Surface contact algorithm.

4 APPLICATION TO KNOTS

Both the Curve-To-Curve (CTC) contact algorithm, see in [3], [7], and the developed Curve-To-Rigid-Surface (CTRS) contact algorithm are used to model the Clove-Hitch knot, see Fig. 5, presented also in [10].

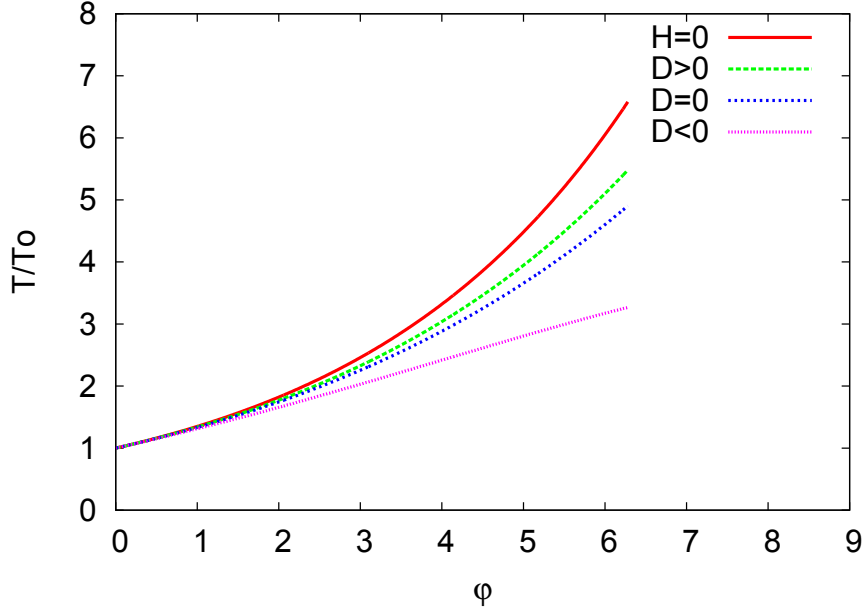


Figure 4: Comparison of all cases with determinant $D > 0$, $D = 0$, $D < 0$ and the classical Euler formula with $H = 0$.

The developed model allows to describe the tying-up mechanics of the Clove Hitch knot: during the tying up both loops of the knot are approaching each other. The upper loop of the knot is enforcing this motion. The knot is tying up and is not slipping because of the large frictional forces appearing between the two approaching loops.

5 CONCLUSIONS

- A special Curve-To-Rigid-Surface (CTRS) contact algorithm is developed in the current contribution based on the application of the Curve-To-Curve contact theory and Segment-To-Analytical Surface (STAS) contact algorithm.
- Rigid surfaces can be approximated with arbitrary NURBS surfaces – in this case an iterative solution of the corresponding Closest Point Projection (CPP) procedure is necessary to define the contact point as well as the penetration.
- An analytical closed form solution for the CPP procedure is possible for some simple cases e.g. for a cylinder.
- The Euler-Eytelwein problem is generalized into the 3D problem as a frictional sliding of a spiral line (helix) on a cylinder. It is shown that consideration of the pitch H leads to the reduction of the force ratio T/T_0 . The formula is used as a basis for the verification of the Curve-To-Rigid-Surface (CTRS) contact algorithm.

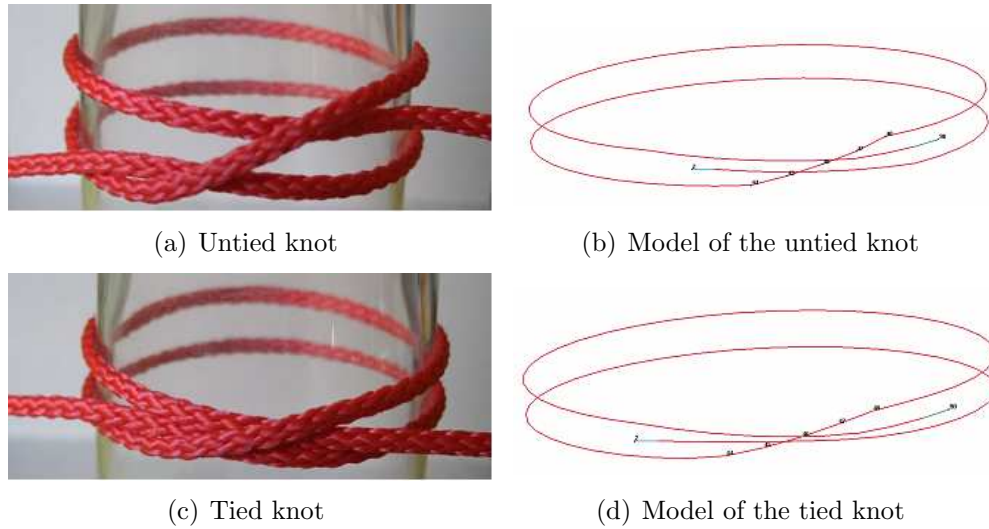


Figure 5: Illustration and finite element model of an untied and tied Clove-Hitch knot

- The developed Curve-To-Rigid (analytical) Surface (CTRS) contact algorithm together with the Curve-To-Curve (CTC) contact algorithm is applied to study the kinematics of the tying up of the Clove Hitch knot.

REFERENCES

- [1] J.A. Cottrell, T.J.R. Hughes and Y. Bazilevs, *Isogeometric Analysis: Toward Integration of CAD and FEA*, John Wiley & Sons, 2009.
- [2] A. Ibrahimbegovic, On finite element implementation of geometrically nonlinear Reissner's beam theory: three-dimensional curved beam elements. *Computer Methods in Applied Mechanics and Engineering* (1995) **122**:11–26.
- [3] Konyukhov A., Schweizerhof K. Geometrically exact covariant approach for contact between curves, *Computer Methods in Applied Mechanics and Engineering* (2010) **199**:2510–2531.
- [4] E. R. Maurer, R. J. Roark, *Technical mechanics: statics, kinematics, kinetics*. -5. ed. New York: Wiley, 1944.
- [5] L. EULER, *Remarques sur l'effet du frottement dans l'équilibre*, Memoires de l'academie des sciences de Berlin, 18 (1769), pp. 265–278.
- [6] J. A. EYTELWEIN, *Handbuch der Statik fester Körper. Mit vorzüglicher Rücksicht auf ihre Anwendung in der Architektur*. Vol. 2, Berlin, 1808, pp. 21–23.
- [7] Konyukhov A., Schweizerhof K. Geometrically exact theory for contact interactions of 1D manifolds. Algorithmic implementation with various finite element models.

Computer Methods in Applied Mechanics and Engineering available online 2 April 2011, doi:10.1016/j.cma.2011.03.013

- [8] Kreyszig E. *Differential geometry*. New York: Dover Publications, 1991.
- [9] Konyukhov A. Geometrically Exact Theory for Contact Interactions, *Habilitationsschrift*, Karlsruhe, KIT, 2010.
- [10] Metzger A., Konyukhov A., Schweizerhof K. Finite element implementation for Euler-Eytelwein-problem and further use in FEM-simulation of common nautical knots. *GAMM, 82nd Annual meeting* 18-21 April 2011, Graz, Austria.
- [11] Konyukhov A., Schweizerhof K. Frictional interaction of a spiral rope and a cylinder – 3D-generalization of the Euler-Eytelwein formula considering pitch. *submitted*.